

PCCP

Accepted Manuscript



This is an *Accepted Manuscript*, which has been through the Royal Society of Chemistry peer review process and has been accepted for publication.

Accepted Manuscripts are published online shortly after acceptance, before technical editing, formatting and proof reading. Using this free service, authors can make their results available to the community, in citable form, before we publish the edited article. We will replace this *Accepted Manuscript* with the edited and formatted *Advance Article* as soon as it is available.

You can find more information about *Accepted Manuscripts* in the [Information for Authors](#).

Please note that technical editing may introduce minor changes to the text and/or graphics, which may alter content. The journal's standard [Terms & Conditions](#) and the [Ethical guidelines](#) still apply. In no event shall the Royal Society of Chemistry be held responsible for any errors or omissions in this *Accepted Manuscript* or any consequences arising from the use of any information it contains.

New trans-stilbene derivatives with large two-photon absorption cross-section and non-linear optical susceptibility values - A theoretical investigation[†]

Varun Kundi^a and Pompozhi Protasis Thankachan^{*a}

Received Xth XXXXXXXXXXXX 20XX, Accepted Xth XXXXXXXXXXXX 20XX

First published on the web Xth XXXXXXXXXXXX 200X

DOI: 10.1039/b000000x

A detailed theoretical study of linear and non-linear optical susceptibilities (NLOS), one- and two-photon absorption (OPA and TPA) properties for a series of push-pull trans-stilbene (TSB) derivatives with introduction of different electron donor (D) and acceptor (A) groups on either side of TSB ring system is presented. The objective of the work is to design new TSB derivatives with large TPA cross-section values and to explore their linear and non-linear optical susceptibilities, OPA and TPA properties. We have used linear and quadratic response theory methods and CAM-B3LYP functional in conjunction with 6-31+G* basis set for all property calculations. We have explained the results of first hyperpolarizability and TP transition probability using two-state model (2SM) calculations, the results of which are in excellent agreement with the response theory methods. The TP tensor elements have been analysed to explain the large TP activity of molecules. Orbitals involved in the transition processes have been studied both qualitatively (molecular orbital pictures) and quantitatively (Λ -values) in order to explain the nature of charge transfer in different TSB derivatives. The study reveals that the novel derivatives TSBD-10, TSBD-11, TSBD-12 and TSBD-13 have large non-linear susceptibilities and TPA cross-section values, the largest being found for TSBD-13 (5560 G.M.).

1 Introduction

Kerr's¹ observation of quadratic electric field induced change in the refractive index in 1875 followed by the discovery of Pockel's effect² in 1883 started the study of non-linear optics of materials. After the invention of laser in 1960 by Maiman,³ the non-linear optical properties of materials came into prominence. Research activity aimed at synthesis and development of noncentrosymmetric molecules with large optical non-linearities has grown motivated by their potential applications in optical and electro optical devices, optical computing, telecommunications, information storage, photodynamic therapy etc.^{4,5} NLO activity has been observed in organic, inorganic and organometallic molecular systems.⁶ Organic molecules are preferred over pure inorganic materials^{7–11} because they are capable of extended π -conjugation which leads to enhanced second order NLO properties, ultra-fast response times, easy tailoring, lower dielectric constants and better process-ability characteristics. Rational design of effective non-linear optical materials depends on the understanding of

hyperpolarizability variation with molecular structure.^{12–15} The broad features of molecules exhibiting better NLO response is a π -conjugated bridge, end capped with strong donor and acceptor substituents. The π -electron cloud movement from donor to acceptor causes the molecule to be highly polarized. The push-pull substituted molecules with extended conjugation have been proven to be the better photon-manipulating materials. The design of new pushpull systems with second-order non-linear optical (NLO) properties has been a subject of great interest over the last few decades. In order to design a chromophore with rapid NLO responses, one can make use of the following three methods¹⁶ (a) Choice of the type of conjugation Bridge along with the number of donor and acceptor substituents and also their strength. (b) Appropriate modification of the nature of conjugation bridge and (c) Increase of the conjugation length in order to alter the NLO response. Electronic factors also play an important role in the strategy for the identification of molecules with large NLO response. In our study, we used a combination of these three strategies to design a set of novel chromophores by choosing suitable donor (D) and acceptor (A) pairs with trans-stilbene (TSB) as a conjugation bridge. The choices were also guided by considerations of thermal stability and blue shifted absorption maxima. The choice of basis set in such studies has been discussed extensively.^{17–21} In 2004, studies²² on third order

^a Theoretical Chemistry Lab, Department of Chemistry, Indian Institute of Technology Roorkee, Roorkee-247667, Uttarakhand, India; E-mail: chemvarun@gmail.com

[†] Electronic Supplementary Information (ESI) available: The optimized Cartesian coordinates of all the systems considered in this work. See DOI: 10.1039/b000000x/

polarizability, using TDDFT, indicated that the split-valence basis set 6-31G is adequate. It was soon seen that for multiconfigurational methods, the 6-31G basis set may lead to completely unrealistic results.²⁰ It is imperative to add the standard polarization (*) and diffuse (+) functions and recent studies¹⁷ suggest that the 6-31+G* basis set is sufficient for estimation of relative hyperpolarisabilities. Hence, we chose the 6-31+G* basis set for our molecular NLO property calculations. The choice of functional for the estimation of molecular NLO properties is also important. Reliable estimation of NLO properties is known to require that the theory level used includes electron correlation. It is known that molecular hyperpolarizability can be reproduced reliably enough using second order Møller-plesset correlation energy correction or coupled cluster methods.^{14,23} However in our study, because of the size of the systems involved, it is not practical to use MP2 or CC methods. Calculations on large molecules using DFT functionals is, on the other hand, quite feasible but the usage of DFT functionals for estimation of molecular NLO properties has come under criticism too.^{24,25} Pure DFT functionals (both local density approximation (LDA) and generalized gradient approximation (GGA)) were found to be inadequate due to wrong asymptotic behaviour of the functional and self-interaction error.¹⁷ These kinds of errors are not present in Hartree-Fock (HF) methods. The inclusion of HF exchange in DFT functionals to form the scaled hybrid functionals reduce the errors involved. Although Hybrid functionals are popular with organic chemists for computing geometries and thermo chemical properties, they failed to predict the impact of electronic fields on molecules.²⁶ The charge transfer resonance states, which are essential to predict hyperpolarisabilities, are also very poorly described by hybrid functionals.²⁶ To avoid these shortcomings, long-range corrected functional, CAMB3LYP, is used in all our calculations, as recommended by recent studies^{27–33} thus evaluating a better description of charge-transfer states. Two-photon activity and first hyperpolarizability, both experimentally and theoretically, of specially 4,4-Dimethyl-amino-nitro-stilbene (TSBD-2) molecule and other TSB derivatives has been investigated extensively by many groups.^{34–36} As per our knowledge, the TSB derivatives studied so far are not having large TPA cross-section values. Our main objective in this work is to design new TSB derivatives with large two-photon absorption (TPA) cross-section and two-photon transition probability. In the present work, we studied thirteen TSB derivatives, out of which four are already known and the rest are newly designed for higher orders of magnitude of hyperpolarizability, two-photon transition probability and TPA cross-section. Therefore, we present here linear and non-linear optical susceptibilities, one- and two-photon absorption properties of these TSB derivatives.

2 Computational details

We performed the gas phase geometry optimizations on all the TSB derivatives using the Kohn-Sham (KS) density functional theory using Gaussian 09 suite of programs³⁷ without using any constraints during the process. Frequency calculations have been performed on all the gas phase optimized geometries and no imaginary frequency was found. The absence of any imaginary frequency ensures that the optimized geometries belong to minima on the potential energy surface. After geometry optimization and frequency calculations, linear polarizability, first and second hyperpolarizability calculations have been performed using DALTON 2013.^{38,39} The one- and two-photon absorption parameters of the first two excited states of all the systems have been calculated using the poles and residues of linear and quadratic response^{40–42} functions in the framework of time-dependent density functional theory (TDDFT), as implemented in the DALTON2013. All the linear and NLOS calculations were carried out using long range corrected Coulomb attenuating method Becke 3-parameters LeeYangParr (CAMB3LYP) functional in conjunction with 6-31+G* basis set. The one- and two-photon calculations were carried out using the CAMB3LYP functional and 6-31+G* basis set. In the long-range corrected CAMB3LYP functional, the B3LYP functional^{43,44} has been modified as

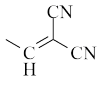
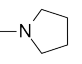
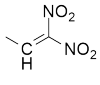
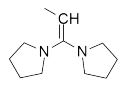
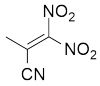
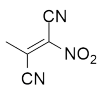
$$\frac{1}{r_{12}} = \frac{1 - [\alpha + \beta \operatorname{erf}(\mu r_{12})]}{r_{12}} + \frac{\alpha + \beta \operatorname{erf}(\mu r_{12})}{r_{12}} \quad (1)$$

In the RHS, the first term, represents the short range interaction and is evaluated by DFT. The second term accounts for the long-range interaction and is evaluated by using Hartree-Fock Exchange. These inequalities *i.e.* $0 \leq \alpha + \beta \leq 1$, $0 \leq \alpha \leq 1$, $0 \leq \beta \leq 1$ are satisfied. Here, the parameter α incorporates the HF exchange contribution over the whole range by a factor α and the parameter β includes the DFT counterpart over the whole range by factor of $1 - (\alpha + \beta)$. The particular choice of CAMB3LYP functional is justified by the fact that it can account for the long-range interaction and can also reproduce experimental excitation energies in charge transfer systems. In this functional, the inter electronic interaction is split into long and short-range parts by an arbitrary parameter. There is only 19% of exact exchange at short-range and 65% at the long-range, and hence, it can account for the long-range interaction in a better way than the conventional hybrid functional. After calculating the first and second hyperpolarizabilities and the one- and two-photon absorption parameters, we have re-evaluated the TPA transition probabilities and first hyperpolarizabilities of all the systems in gas phase using the two-state-model (2SM) approach. The parameters required for 2SM calculations have been calculated using the double residue of quadratic response theory of the DALTON2013 package.

3 Results and Discussion

We have designed the TSB derivatives for study taking different combinations of donor and acceptor moieties as given in Table 1. The gas phase optimized geometries and corresponding reaction coordinates are supplied in **ESI**. The molecules considered in study are named as TSBD-n (n=1, 2, 3, ..., 13) and belong to C1 point group.

Table 1 A two-dimensional pictorial representation of the basic skeleton of the systems, their nomenclature and different donor–acceptor groups.

TSB Derivative						
System	Combinations	Donor (D)	Donor (D)	Acceptor (A)	Acceptor (A)	
TSBD-1	D=D1 A=A1	D1	–NH ₂	A1	–NO ₂	
TSBD-2	D=D2 A=A1					
TSBD-3	D=D3 A=A1	D2	–N(CH ₃) ₂	A2	–CN	
TSBD-4	D=D4 A=A1					
TSBD-5	D=D5 A=A1	D3	–N(C ₂ H ₅) ₂	A3		
TSBD-6	D=D6 A=A1					
TSBD-7	D=D1 A=A2	D4		A4		
TSBD-8	D=D1 A=A3					
TSBD-9	D=D1 A=A4	D5		A5		
TSBD-10	D=D5 A=A4					
TSBD-11	D=D5 A=A3	D6	–OCH ₃	A6		
TSBD-12	D=D5 A=A5					
TSBD-13	D=D5 A=A6					

3.1 Geometry of the systems

To begin with let us compare our optimized geometries with previously reported results from experimental and computational studies. Some selected geometrical parameters of TSB and TSBD-2 (DANS (4, 4-dimethyl-amino-nitro-stilbene)) are provided in **ESI**. It is seen that the experimental parameters reported for TSB (with parenthesis) differ from our results at the most 0.023 Å (C1–C1') or 0.76° (C1–C1'–C2') while the difference with the computational results of Alam et. al.³⁴ is only in the third place of decimals for distances. In view of this, we optimized our all the TSB derivatives at B3LYP/6-31G (d) level of theory in order to reduce the computational cost.

3.2 Linear and Non Linear Polarizability

In the present work we have calculated the isotropic average polarizability ($\langle\alpha\rangle$), static first hyperpolarizability (β_{tot}) and second hyperpolarizability ($\gamma_{||}$) values of all the TSB derivatives shown in Table 2. The relationship between the spatial components of induced dipole moment μ_i and the components of electric field E_j which creates it, shows the existence of NLO phenomena at the microscopic level. When a molecule is placed in an electric field of strength E , its dipole moment can be expanded in a Taylor's series in powers of the field strength as:

$$\mu_i = \mu_i^o + \alpha_{ij}E_j + \beta_{ijk}E_jE_k + \gamma_{ijkl}E_jE_kE_l + \dots \quad (2)$$

where μ_i^o is the dipole moment of the unperturbed molecule (permanent dipole moment), α_{ij} is the linear polarizability, β_{ijk} and γ_{ijkl} are the first and second hyperpolarisabilities, respectively and the summation convention has been used. The linear polarizability, first hyperpolarizability and second hyperpolarizability tensor components are obtained as the first, second and third derivatives of the dipole moment with respect to applied field as

$$\alpha_{ij} = \left(\frac{\partial \mu_i}{\partial E_j} \right)_{E=0}, \beta_{ijk} = \left(\frac{\partial^2 \mu_i}{\partial E_j \partial E_k} \right)_{E=0}, \gamma_{ijkl} = \left(\frac{\partial^3 \mu_i}{\partial E_j \partial E_k \partial E_l} \right)_{E=0}$$

The isotropic average polarizability ($\langle\alpha\rangle$) is defined as

$$\langle\alpha\rangle = \frac{(\alpha_{xx} + \alpha_{yy} + \alpha_{zz})}{3} \quad (3)$$

We can calculate the components of β using the equation

$$\beta_i = \beta_{iii} + \frac{1}{3} \sum_{i \neq j} (\beta_{ijj} + \beta_{jij} + \beta_{jji}) \quad (4)$$

β_{tot} , is given by

$$\beta_{tot} = (\beta_x^2 + \beta_y^2 + \beta_z^2)^{\frac{1}{2}} \quad (5)$$

The hyperpolarizability is a third-rank tensor with $3 \times 3 \times 3 = 27$ components. These can be reduced to 10 because of the Kleinman symmetry ($\beta_{xyy} = \beta_{yyx} = \beta_{yxy}$, $\beta_{yyz} = \beta_{zyy} = \beta_{zyz} \dots etc.$) and expressed in a lower tetrahedral format. Out of 21 tensor components of second hyperpolarizability, 18 components satisfy the following relationship.

$$\begin{aligned} \gamma_{xxy} &= \gamma_{yyx} = \gamma_{xyx} = \gamma_{yxx} = \gamma_{xyx} = \gamma_{xyx} \\ \gamma_{xxx} &= \gamma_{zxx} = \gamma_{xzx} = \gamma_{zxx} = \gamma_{zxx} = \gamma_{zxx} \\ \gamma_{yyz} &= \gamma_{zzy} = \gamma_{zyz} = \gamma_{zyz} = \gamma_{zyz} = \gamma_{zyz} \end{aligned}$$

Therefore, the averaged gamma parallel to the applied field can be expressed as

$$\gamma_{\parallel} = \frac{1}{5} (\gamma_{xxxx} + \gamma_{yyyy} + \gamma_{zzzz} + 2\gamma_{xxyy} + 2\gamma_{xxzz} + 2\gamma_{yyzz}) \quad (6)$$

The molecules considered in our study show asymmetric polarization which is induced by electron donor and acceptor in the π -conjugated systems. We tried to compare the electronic effects on the first, second and third order polarizability of TSB upon substitution of donor and acceptor groups. The values of isotropic average polarizability ($\langle\alpha\rangle$), total first hyperpolarizability (β_{rot}) and second hyperpolarizability (γ_{\parallel}) calculated for all molecules under investigation at CAMB3LYP level are given in Table 2. As we can see from that the isotropic average polarizability goes on increasing from TSBD-1 to TSBD-5. A similar relative trend is shown by the non-linear optical susceptibilities (NLOS) i.e. first and second hyperpolarizabilities. From TSBD-1 to TSBD-5, the acceptor group (-NO₂) is same and the variation of donor group is responsible for the change in linear and non-linear optical susceptibilities. This is attributed to the increasing positive inductive effect (+I) as we move from TSBD-1 to TSBD-5. We can clearly see that as we move from TSBD-1 to TSBD-4, pyrrolidine (D4) is proven to be the best donor therefore, we tried to attach two pyrrolidine rings through the introduction of one more double bond as shown in Table 1, thereby generating TSBD-5 which led to the significant increase in linear and non-linear optical susceptibilities as compared to the TSBD-4. This enhanced linear and NLOS is due to the introduction of double bond, thereby increasing conjugation and two pyrrolidine rings. The NLOS of TSBD-6 is lower than the TSBD-1 only because of the poor donor strength of D6 than D1 as expected. From the system TSBD-7 to TSBD-9, we tried a variation in the acceptor group. As seen from NLOS value of TSBD-7, it indicates that A2 is a poor acceptor as compared to A1, so in order to increase the value NLOS significantly we introduced a double bond which helped us to attach two A2 groups. As A1 is a better acceptor than A2, we replaced both A2s with A1s and got higher NLOS value with significant difference from the previous system. TSBD-10 and TSBD-11 are designed with best donor group (D5) from the studied donors and A3, A4 as acceptors respectively. TSBD-12 and TSBD-13 are the systems with very high NLOS values as compared to previous systems. We modified A4 by the introduction of a CN group replacing the H attached to the C atom which is directly attached to the benzene ring of TSB. There is also small increase in the value of NLOS when -NO₂ group trans to CN is replaced by the -CN. This may be due to the reason that -NO₂ group causes the steric repulsions and disturbs the orientation of other groups. The enhanced values of NLOS for TSBD-12 and TSBD-13 have proven themselves as the best

candidates for the NLO application and D5 and A6 as best donor and acceptor respectively from the studied donors and acceptors.

To understand this phenomenon in context of molecular orbitals, we examined energies of highest occupied molecular orbital (HOMO) and lowest occupied molecular orbital (LUMO). The results of all the systems are shown in Fig. 1. We can see that as the donor strength goes on increasing in compounds TSBD-1 to TSBD-5 keeping the same acceptor group, the E_{HOMO} goes on increasing and E_{LUMO} remains essentially the same. Therefore, HOMO-LUMO gap keeps decreasing resulting in increase of NLOS and therefore ICT from donor to acceptor. The substitution of D6 (OCH₃) group for D1 (-NH₂) drastically reduced the energy of HOMO keeping the LUMO at comparatively same level thereby increasing the gap leading to smaller NLOS value. Substitution of A2 (-CN) group in place of A1 (-NO₂) in TSBD-7 has drastically increased the LUMO level thereby decreasing the NLOS value. E_{LUMO} is now decreasing in TSBD-8 and TSBD-9 due to the variation in acceptor (A3 and A4) keeping E_{HOMO} similar with same donor (D1). From TSBD-9 to TSBD-10, due to the substitution of D1 with D5 (relatively strong donor), E_{HOMO} has been increased significantly maintaining E_{LUMO} at same position because of same acceptor (A4) lead to decrease the gap and increase in NLOS value. E_{HOMO} is similar in remaining systems with change in E_{LUMO} values due to the variation in acceptors thereby leading to the significant changes in NLOS values. For the quantitative description of the trends followed by NLOS, we also applied two-state model (2SM) for the calculation of static first hyperpolarizability by using sum-over-state (SOS) perturbation procedure. Thus, value of β is reduced to simple expression:⁴⁵

$$\beta_{(0;0,0)}^{2SM} = 3\Delta\mu^{ff} \frac{\mu_{if}^2}{\omega_{if}^2} \quad (7)$$

where ω_{if} , μ_{if} and $\Delta\mu^{ff}$ are excitation energy, transition dipole moment vector and difference in dipole moments between the involved states (i, f). In 2SM, we have considered ground state ($|0\rangle$) and first excited state ($|1\rangle$) in the SOS equations. Here we can clearly see the strong dependence of β on the transition dipole moment vector and difference in dipole moments between ground and first excited state and inversely related to the excitation energy. We can clearly see that the 2SM results are in very good agreement with the response theory results. Here, we can make quantitative discussions because we have the values of all the quantities on which β depends very strongly. The magnitude of β goes on increasing as we move from TSBD-1 to TSBD-5. This is clearly due to the continuous increment in the values of μ_{01} and $\Delta\mu^{11}$ and decrement in the ω_{01} values. The difference between the first and second hyperpolarizability values of (TSBD-1, TSBD-2) pair is more than the differences between (TSBD-2, TSBD-3) and

Table 2 Isotropic polarizability ($\langle\alpha\rangle$), static first hyperpolarizability (β_{tot}) and second hyperpolarizability ($\gamma_{||}$) of all the systems in Gas phase calculated at CAMB3LYP/6-31+G* level of theory: ω_{01} = Excitation energy, μ^{01} = Norm of ground ($|0\rangle$) to first excited ($|1\rangle$) state transition dipole moment vector, $\Delta\mu^{11}$ = Dipole moment difference between the ground ($|0\rangle$) and first excited ($|1\rangle$) state and β^{2SM} = static first hyperpolarizability using two-state model approach.

System	$\langle\alpha\rangle$ (a.u.)	β_{tot} (10^3 a.u.)	$\gamma_{ }$ (10^5 a.u.)	ω_{01} (a.u.)	μ^{01} (a.u.)	$\Delta\mu^{11}$ (a.u.)	β^{2SM} (10^3 a.u.)
TSBD-1	236.71	12.36	5.40	0.1256	3.694	4.158	10.79
TSBD-2	273.84	17.43	8.08	0.1200	3.906	4.832	15.35
TSBD-3	300.43	18.52	8.87	0.1199	3.982	4.963	16.42
TSBD-4	301.31	19.95	9.54	0.1182	4.035	5.003	17.84
TSBD-5	415.34	33.87	20.82	0.1078	4.548	5.897	31.50
TSBD-6	239.07	9.87	4.53	0.1305	3.640	3.842	8.96
TSBD-7	231.54	7.48	3.54	0.1348	3.729	2.472	5.67
TSBD-8	318.64	23.08	11.33	0.1137	4.505	4.130	19.46
TSBD-9	323.33	29.85	14.77	0.1099	4.364	5.254	24.86
TSBD-10	527.75	78.53	56.96	0.0939	5.127	7.903	70.68
TSBD-11	517.07	61.98	42.70	0.0980	5.236	6.561	56.23
TSBD-12	572.91	125.13	104.73	0.0795	4.680	9.538	99.19
TSBD-13	589.37	133.72	104.10	0.0783	4.941	8.653	103.31

(TSBD-3, TSBD-4) pairs because the values of μ_{01} and $\Delta\mu^{11}$ and ω_{01} are varying in similar proportion to the magnitude of NLOS. While moving from TSBD-6 to TSBD-7, TSBD-8 to TSBD-9 and TSBD-10 to TSBD-11, it is $\Delta\mu^{11}$ which is controlling the $\beta_{(0;0,0)}^{2SM}$ by varying its value more or less in order to develop good agreement with response theory results.

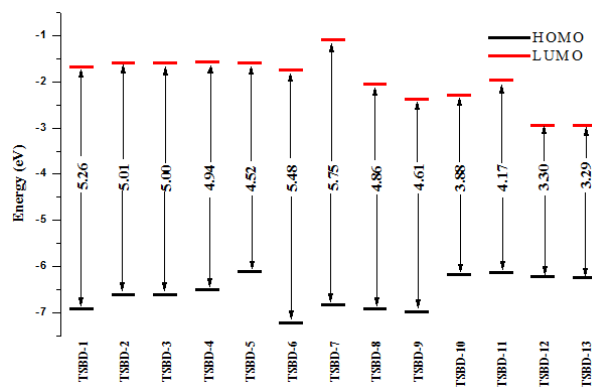


Fig. 1 Changes in the energy levels of HOMO-LUMO

3.3 One Photon Absorption Process

Let us now discuss the OPA process for all the TSB derivatives in this context. The oscillator strength (δ_{OPA}) gives the probability of transition from one state to another state by absorption of single photon of incident light. For the transition from one state (say i) to another state (say f) with excitation energy ω_{if} , the oscillator strength is given by⁴⁶

$$\delta_{OPA} = \frac{2\omega_{if}}{3} \sum_{\alpha} |\langle i | \mu_{\alpha} | f \rangle|^2 \quad (8)$$

Where $\alpha \in \{x, y, z\}$ and μ_{α} is the α th component of dipole moment operator. We have considered the first two excited states of each molecule in this study for the investigation of OPA activity of these states. The OPA data for the first two excited states are given in Table 3.

We find that the first excited state of all the TSB derivatives is OP active with a large value of oscillator strength (δ_{OPA}). The second excited state of systems from TSBD-1 to TSBD-6 are OPA inactive with extremely small values of δ_{OPA} , whereas the systems from TSBD-7 to TSBD-13 have small values of oscillator strength but larger than those of the former set. These results can be explained by taking the values of μ_{of} and ω_{of} into account. We can clearly see that the values of μ_{of} follow the same trend as δ_{OPA} . From TSBD-1 to TSBD-6, μ_{of} values for the second excited state are very small and follow the same trend as δ_{OPA} values whereas values of ω_{of} remain almost the same. Therefore, only μ_{of} plays a role in controlling the OP activity of the derivatives studied. It has also been reported in earlier studies that the trend followed by δ_{OPA} is not influenced by ω_{of} . Gas phase ω_{of} value, 3.27 eV of TSBD-2 is close to the experimentally reported⁴⁷ value 3.69 eV and very close to the earlier theoretically reported⁴⁸ value 3.39 eV. The value of μ_{of} (3.91 a.u.) of TSBD-2 is also in excellent agreement with the theoretically reported value of 3.89 a.u..⁴⁸ In order to have a microscopic view at the nature of the transition in all the TSB derivatives, the study of different contributing orbitals has been performed. The orbital pictures are shown in Fig. 2. It is noticed that $S_0 \rightarrow S_1$ transition

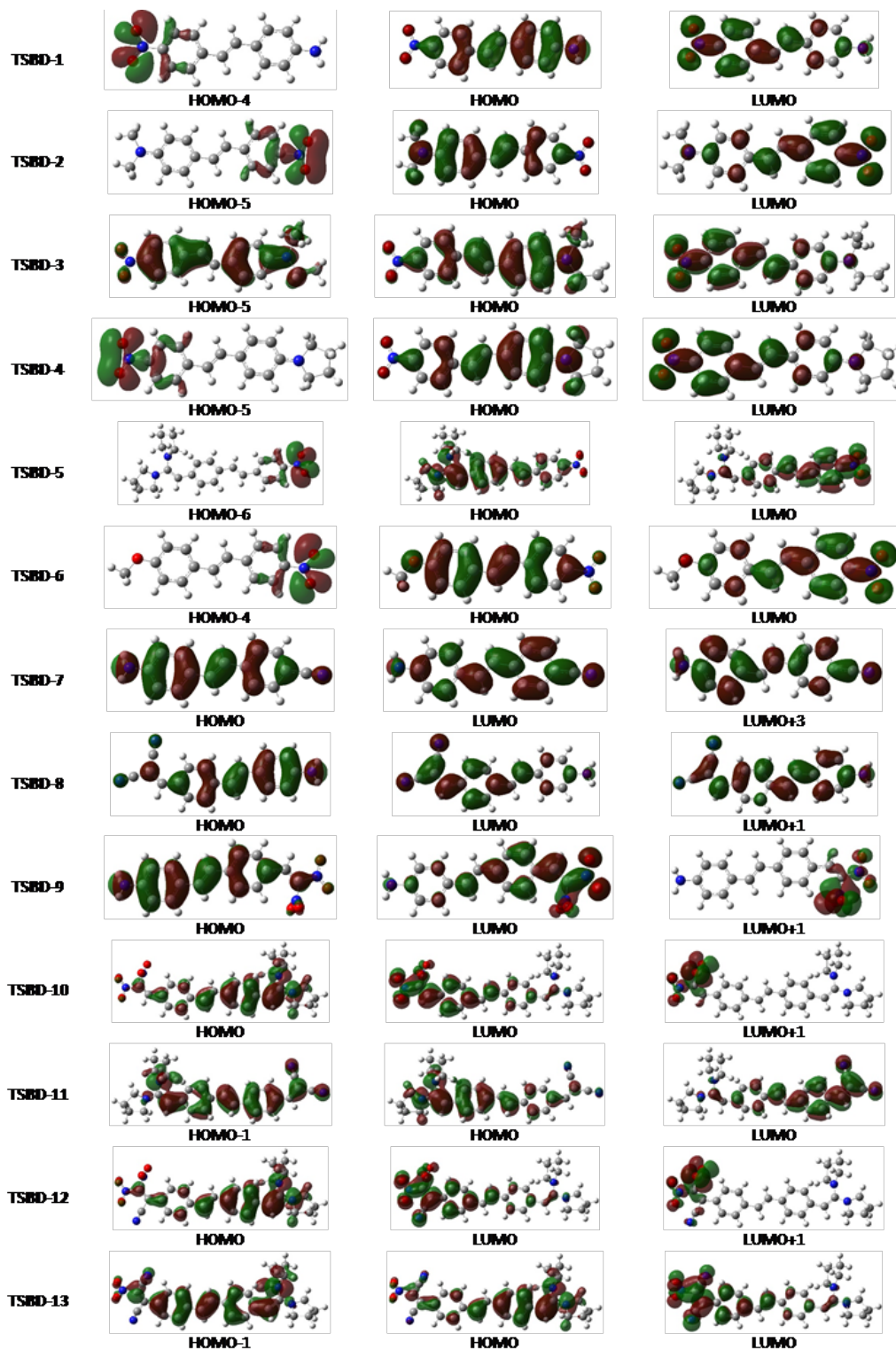


Fig. 2 Orbital involved in $S_0 \rightarrow S_1$ and $S_0 \rightarrow S_2$ transitions in the studied molecules - The x-axis is perpendicular to the plain of the paper

Table 3 OPA parameters of first two excited states of all the systems in Gas phase calculated at CAMB3LYP/6-31+G* level of theory: ω_{0i} = Excitation energy, μ^{0i} = Norm of ground ($|0\rangle$) to excited ($|i\rangle$) state transition dipole moment vector, δ_{OPA} = oscillator strength, H = HOMO, L = LUMO; in last column the first entry in parenthesis is the weight and second entry represents the contribution of the orbital pair in the corresponding transitions

System	Excited States (i)	ω_{0i} (a.u.)	μ_{0i} (a.u.)	δ_{OPA}	Λ	Orbital transitions
TSBD-1	1	0.1256	3.694	1.143	0.546	H \rightarrow L (0.393, 0.210)
	2	0.1415	0.003	0.000	0.370	H-4 \rightarrow L (0.355, 0.143)
TSBD-2	1	0.1200	3.906	1.221	0.506	H \rightarrow L (0.389, 0.190)
	2	0.1416	0.002	0.000	0.373	H-5 \rightarrow L (0.358, 0.145)
TSBD-3	1	0.1199	3.982	1.267	0.503	H \rightarrow L (0.389, 0.189)
	2	0.1415	0.010	0.000	0.376	H-5 \rightarrow L (0.358, 0.146)
TSBD-4	1	0.1182	4.035	1.283	0.500	H \rightarrow L (0.390, 0.188)
	2	0.1415	0.001	0.000	0.374	H-5 \rightarrow L (0.360, 0.146)
TSBD-5	1	0.1078	4.548	1.486	0.456	H \rightarrow L (0.365, 0.155)
	2	0.1414	0.009	0.000	0.362	H-6 \rightarrow L (0.344, 0.138)
TSBD-6	1	0.1305	3.640	1.153	0.573	H \rightarrow L (0.397, 0.226)
	2	0.1416	0.000	0.000	0.370	H-4 \rightarrow L (0.352, 0.141)
TSBD-7	1	0.1348	3.729	1.250	0.695	H \rightarrow L (0.407, 0.289)
	2	0.1674	0.716	0.043	0.562	H \rightarrow L+3 (0.194, 0.130)
TSBD-8	1	0.1137	4.505	1.538	0.573	H \rightarrow L (0.396, 0.223)
	2	0.1592	0.446	0.021	0.631	H \rightarrow L+1 (0.198, 0.146)
TSBD-9	1	0.1099	4.364	1.394	0.484	H \rightarrow L (0.382, 0.176)
	2	0.1281	0.703	0.039	0.256	H \rightarrow L+1 (0.162, 0.018)
TSBD-10	1	0.0939	5.127	1.645	0.400	H \rightarrow L (0.372, 0.133)
	2	0.1235	0.476	0.014	0.181	H \rightarrow L+1 (0.195, 0.014)
TSBD-11	1	0.0980	5.236	1.790	0.466	H \rightarrow L (0.377, 0.162)
	2	0.1403	0.915	0.066	0.641	H-1 \rightarrow L (0.183, 0.126)
TSBD-12	1	0.0795	4.680	1.160	0.339	H \rightarrow L (0.405, 0.127)
	2	0.1178	0.562	0.018	0.144	H \rightarrow L+1 (0.300, 0.022)
TSBD-13	1	0.0783	4.940	1.272	0.369	H \rightarrow L (0.401, 0.138)
	2	0.1209	2.400	0.448	0.500	H-1 \rightarrow L (0.291, 0.147)

in all the TSB derivatives is dominated by highest occupied molecular orbital (HOMO)-lowest unoccupied molecular orbital (LUMO) pair. We can clearly see from the orbital picture that the electron densities in TSBD-1 to TSBD-6, TSBD-8, TSBD-9 and TSBD-11 are spread over the whole molecule and not on the particular donor and acceptor. This concludes the mixing of charge transfer and π -electron reorganization phenomenon. For the $S_0 \rightarrow S_2$ transition, the dominant molecular orbital pairs for all the derivatives are also reported in Table 2. The OP inactivity of second excited state for TSBD-1 to TSBD-6 can also be explained from the orbital picture. By careful analysis, we find that in all the six molecules (TSBD-1 to TSBD-6) the electron density is spread around acceptor in both the significant orbitals with dominant contribution for $S_0 \rightarrow S_2$ transition. The almost zero participation of orbitals from donor side led to the OP inactivity of the second excited state. From TSBD-7 to TSBD-13, the δ_{OPA} has larger values compared to the former set thereby making the second excited state OP active. This can also be explained from orbital pictures by analyzing the concerned orbitals mentioned in Table 3 with dominant contributions for $S_0 \rightarrow S_2$ transition. This OP activity is due to the fact that during transition, the charge is being transferred from donor part of molecule to the acceptor part along with π -electron reorganization. We can clearly see that the Λ -parameter can quantitatively differentiate the short and long-range nature of the transition in a molecule. Therefore we have further calculated the well-established Λ -parameter^{49–53} for supporting the orbital picture results. Λ is defined using the inner product (ϑ_{ia}) between all the pairs of occupied (i) and virtual orbitals (a) involved in the transition and weighted by some function (κ_{ia}). It is given by⁵⁴ as

$$\Lambda = \frac{\sum_{i,a} \kappa_{ia}^2 \vartheta_{ia}}{\sum_{i,a} \kappa_{ia}^2} \quad (9)$$

where the function κ_{ia} is defined as the sum of solution vectors of the basic TDDFT equation within adiabatic approximation. The value of Λ lies between 0 and 1. Long range transitions are characterized by smaller values of Λ . This has been used by the several authors in order to explain the short range and long range nature of transitions in the molecule. Peach et al.⁵⁴ have found a large value of Λ (0.72) for DMABN molecule. Similarly, Chattopadhyaya et al.⁵⁵ have reported a value of 0.88 for bisanthene molecule where the transition is essentially of short-range nature. Chakrabarti and Ruud have noticed a very small value of Λ (0.16) for a through space charge-transfer system tweezerTNF complex.⁵⁶ Recently, Alam et al.^{50,57,58} have found a value of 0.2 for a double positively charged [2, 2] paracyclophane derivative, 0.7 for p-betaine, and 0.5 for o-betaine and boronnitrogen containing charge transfer systems. In our study, for $S_0 \rightarrow S_1$ transition, the systems TSBD-1 to TSBD-6, TSBD-8, TSBD-9 and TSBD-11 have Λ values around 0.5 as shown in Table

3. Therefore all these molecules fall in the category of mixing of charge transfer and π -electron reorganisation phenomena rather than only charge transfer. The maximum Λ value (0.695) obtained amongst all the TSB derivatives under investigation is for TSBD-7. This shows a short range transition whereas the molecule TSBD-12 has Λ value for the first excited state is 0.339 and for second excited state is 0.144. The nature of transition for TSBD-12 to the first excited state is slightly inclined towards long range nature whereas the transition to the second excited state is clearly long range in nature, in which the participating orbitals are HOMO and LUMO+1. This result supports the orbital pictures in which the electron density is concentrated only on the acceptor group. A similar situation can also be seen for the second excited state of TSBD-9. Therefore, on the basis of both the nature of orbitals involved and the value of Λ parameter, we may conclude that the transition to first excited state of all the TSB derivatives except TSBD-7, TSBD-10, TSBD-12 and TSBD-13 is a mixture of charge-transfer and π -electron reorganization process. The transition involved in TSBD-7 is short range in nature whereas in TSBD-10, TSBD-12 and TSBD-13 it is slightly inclined towards long range in nature. Moreover, the linear relationship between Λ -values and two photon absorption cross section, as discussed by Murugan *et al.*⁵⁹, can also be seen in the present study. (Figure 2. showing the linear relationship has been shown in ESI)

3.4 Two-photon Absorption Process

For the linearly polarised light, the TP transition probability, which is characteristic of TPA process theoretically, is given by^{60–63}

$$\delta_{TPA} = \sum_{\alpha,\beta} (2S_{\alpha\alpha}S_{\beta\beta} + 4S_{\alpha\beta}^2) \quad (10)$$

Where $S_{\alpha\beta}$ are the TP tensor components and the indices α , β run over the coordinate axes x, y and z. The TP tensor element, $S_{\alpha\beta}$ is related to the various transition moment integrals and excitation energies by the relationship^{60–63}

$$S_{\alpha\beta} = \sum_i \frac{\mu_{\alpha}^{0i} \mu_{\beta}^{if} + \mu_{\beta}^{0i} \mu_{\alpha}^{if}}{\omega_{0i} - \omega_{of}/2} \quad (11)$$

Where μ and ω are having the same meanings as in equation 8. Before discussing the TPA results, it is important to mention here is that we have used CAMB3LYP/6-31+G* level of theory for TPA calculation. This basis set may seem to be the smaller one but we also performed the TPA calculation on TSBD-2 with cc-pVDZ, aug-cc-pVDZ basis sets and also compared the results with Alam et al.³⁴ We have seen that the values obtained with aug-cc-pVDZ and 6-31+G* are very close whereas with cc-pVDZ basis set the values are smaller

but the order of magnitude is same in all three basis sets used. In view of this, we used 6-31+G* basis set for TPA calculations. TPA calculations have been performed for the first two excited states of all the TSB derivatives using quadratic response theory. The δ_{TP} results from the response theory are represented as δ_{TP}^{Resp} . The TPA cross section values can be calculated using the following relationship^{59c}

$$\sigma_{TPA} = \frac{(2\pi)^3 \alpha a_0^5 \omega^2}{c\pi\Gamma} \delta_{au} \quad (12)$$

where α is the fine structure constant; a_0 is the Bohr radius; Γ is the width of the Lorentzian shape absorption profile; ω is the energy of photon and c is speed of light. Γ is chosen to be 0.1 eV as motivated from the previous studies.^{64,65} The results for δ_{TP}^{Resp} and $S_{\alpha\beta}$ are presented in Table 4. It is important to note that the first excited state of all the TSB derivatives is TPA active, whereas the second excited state of TSBD-1 to TSBD-6 is TPA inactive and the remaining are TPA active with a lower order of magnitude as compared to the corresponding first excited state δ_{TP}^{Resp} values. The second excited state of TSBD-13 is highly TP active with the highest δ_{TP}^{Resp} value (70×10^4 a.u.) and TPA cross-section (5560 GM). The first excited state is also highly TP active but with lower δ_{TP}^{Resp} (68.1×10^4 a.u.) and TPA cross-section (2270 GM) values in comparison with the second excited state. On comparing all the studied TSB derivatives, TSBD-10, TSBD-12 and TSBD-13 have higher transition probability values and TSBD-7 has the smallest TP value (1.13×10^4 a.u.) for the first TP active state. For the first excited state, the relative trend of δ_{TP}^{Resp} and TPA cross-section values followed by the TSB derivatives under investigation is similar to that followed by first and second hyperpolarizabilities due to their dependence on different combinations of donor and acceptor groups as discussed earlier in the section on linear and non-linear susceptibility, whereas for the second excited state, these trends are not similar to those of first and second hyperpolarizabilities. For a detailed examination of their TP activity, an analysis of six unique TP tensor elements has also been performed. We can clearly see that for TP inactive states of all the TSB derivatives under study, all the TP tensor elements are either zero or very low (close to zero). It has been noticed that the major contributing tensor component for the first excited state of all the TSB derivatives is S_{zz} . As the donor and acceptor are oriented in z-direction therefore S_{zz} is the dominant factor in TP activity of the first excited state for all the TSB derivatives. The direction of charge transfer which is responsible for TPA activity is also indicated by the major contributing tensor element. In order to rationalize this TP activity of all the TSB derivatives, we have performed two-state model (2SM) calculations, within GFSM for 3D molecules. Within 2SM, the expression for δ^{2SM} is given by⁵⁷

$$S_{\alpha\beta}^{2SM} = \frac{2(\mu_{\alpha}^{0f} \Delta\mu_{\beta}^{ff} + \mu_{\beta}^{0f} \Delta\mu_{\alpha}^{ff})}{\omega_{0f}} \quad (13)$$

$$\delta_{TPA}^{2SM} = 8 \left(\frac{2\mu^{0f} \Delta\mu^{ff}}{\omega_{0f}} \right)^2 (2\cos^2\theta + 1) \quad (14)$$

Where θ is the angle between μ^{0f} and $\Delta\mu^{ff}$ vectors and μ , ω terms have their usual meanings. The results of 2SM calculations have also been provided in Table 4. We can see that the value of θ for the first excited state of all the TSB derivatives is close to 180° or 0° . Therefore the value of angle dependent term $(2\cos^2\theta + 1)$ is close to +3. The TP inactivity of the second excited state of systems from TSBD-1 to TSBD-6 points towards the very low (close to zero) values of μ^{0f} regardless the values of $\Delta\mu^{ff}$ and other factors involved in equation 13. For the first excited state, the relative trend followed by δ^{2SM} values for all the TSB derivatives is similar to that of the followed by the δ_{TP}^{Resp} with ratio of δ^{2SM} to δ_{TP}^{Resp} for all the TSB derivatives falling between 1.3 and 1.5. As we move from TSBD-1 to TSBD-6, μ^{0f} and $\Delta\mu^{ff}$ follow the same trend as that of followed by δ_{TP}^{Resp} and δ^{2SM} . From Table 4 it is clearly seen that δ_{TP}^{Resp} and δ^{2SM} go on increasing from TSBD-1 to TSBD-5. The important thing to be noticed here is that though both the factors, μ^{0f} and $\Delta\mu^{ff}$ are increasing, the increment in μ^{0f} is less than the increment in $\Delta\mu^{ff}$. Therefore, the increment of $\Delta\mu^{ff}$ is contributing more in order to increase the δ^{2SM} proportionally to the increase in δ_{TP}^{Resp} . A similar situation is also seen when we move from TSBD-5 to TSBD-6, where the decrement in $\Delta\mu^{ff}$ is more than μ^{0f} so as to reach up to the proportional value. In the cases of movement from TSBD-6 to TSBD-7, TSBD-10 to TSBD-11 and TSBD-12 to TSBD-13, the δ_{TP}^{Resp} , δ^{2SM} values are decreasing while μ^{0f} values are increasing. Therefore, to maintain the trend of δ_{TP}^{Resp} and δ^{2SM} similar, $\Delta\mu^{ff}$ is decreasing more thereby overpowering the opposing effects created by μ^{0f} . Similar is the case when we go from TSBD-11 to TSBD-12, but in opposite sense to the previously discussed case. Here we can see that in all the cases (ups and downs) ω_{0f} is acting in favour of $\Delta\mu^{ff}$ except while moving from TSBD-12 to TSBD-13 where ω_{0f} should increase but decreasing. Therefore, in view of the above discussion, we can say that it is the changes of $\Delta\mu^{ff}$ which controls the values of δ^{2SM} . A careful investigation of the components of the vectors involved indicates that the z-component is the dominant element for all the TSBD-derivatives under study thereby making S_{zz} the main contributing tensor element of all.

4 Conclusions

We have used response theory to study gas phase linear and non-linear optical susceptibilities, one- and two-photon ab-

Table 4 TPA parameters and TP tensor elements of first two excited states of all the systems in Gas phase calculated at CAMB3LYP/6-31+G* level of theory: $\Delta\mu^{ff}$ = Dipole moment difference between the ground ($|0\rangle$) and excited ($|i\rangle$) states, θ = Angle between the μ^{0f} and $\Delta\mu^{ff}$ vectors

System	Excited states (i)	S_{xx}	S_{yy}	S_{zz}	S_{xy}	S_{xz}	S_{yz}	$\Delta\mu^{ff}$ (a.u.)	θ (degree)	δ_{TPA}^{2SM} (10^4 a.u.)	$\delta_{TPA}^{Resp.}$ (10^4 a.u.)	σ_{TPA} (G.M.)
TSBD-1	1	-0.4	-5.0	406.5	0.0	-0.8	5.0	4.158	178.76	4.78	3.28	281
	2	0.0	0.0	0.2	0.3	0.1	0.0	1.058	5.27	0	0	0
TSBD-2	1	-1.0	-6.6	520.6	0.0	0.2	3.5	4.832	179.05	7.91	5.37	420
	2	0.0	0.0	-0.2	0.3	0.1	0.0	1.095	176.41	0	0	0
TSBD-3	1	0.7	6.1	-544.0	1.2	4.7	0.8	4.963	1.18	8.69	5.87	458
	2	0.1	-0.2	0.9	0.3	0.1	0.0	1.106	2.23	0	0	0
TSBD-4	1	1.0	6.8	-565.9	0.4	0.4	-0.2	5.003	0.86	9.33	6.35	481
	2	0.0	0.0	0.0	-0.3	0.1	0.0	1.115	9.41	0	0	0
TSBD-5	1	-2.7	-0.4	802.5	-2.3	-8.7	-21.6	5.897	177.69	19.8	12.90	811
	2	-0.3	0.3	2.9	-0.1	-0.1	-0.2	1.188	164.89	0	1.68	0
TSBD-6	1	-0.4	-4.9	352.7	0.0	0.0	4.7	3.842	178.05	3.67	2.46	228
	2	0.0	0.0	0.0	-0.3	0.1	0.0	1.044	2.66	0	0	0
TSBD-7	1	0.2	-3.7	239.0	0.0	0.8	1.4	2.472	179.58	1.50	1.13	112
	2	0.7	3.7	-74.0	0.5	-0.1	-13.7	0.340	154.03	5.92	0.11	16.8
TSBD-8	1	0.2	3.1	-548.5	0.0	0.8	3.9	4.130	0.96	8.57	5.99	420
	2	-0.7	6.1	15.4	0.1	0.9	24.3	1.248	89.16	13.1	0.02	3.06
TSBD-9	1	0.6	2.8	-695.6	-0.4	3.5	31.9	5.254	0.16	13.9	9.67	634
	2	0.0	6.6	-120.4	0.3	1.3	28.1	3.301	33.95	0.08	0.30	26.8
TSBD-10	1	-1.5	-1.7	1388.6	2.0	12.6	0.7	7.903	178.93	59.6	38.5	1840
	2	1.7	7.3	-87.1	-3.8	-18.4	42.3	6.237	46.21	0.12	0.20	16.5
TSBD-11	1	1.5	-0.4	-1139.1	1.6	6.5	26.6	6.561	0.53	39.4	26.0	1350
	2	2.4	0.2	-1.1	3.1	-13.7	-65.0	2.943	112.07	0.05	0.12	12.6
TSBD-12	1	-0.8	-1.6	1864.7	1.7	10.8	45.0	9.538	179.18	101.0	69.5	2380
	2	-4.9	-7.5	380.4	7.2	61.2	-58.1	9.013	133.92	0.39	3.0	228
TSBD-13	1	1.4	1.3	-1843.8	-1.9	14.0	-69.8	8.653	1.34	95.3	68.1	2270
	2	2.0	2.2	1869.6	-0.8	-6.3	25.4	7.939	9.24	7.81	70.0	5560

sorption properties of TSB derivatives. We used two-state model approach in order to re-evaluate the first hyperpolarizabilities and two-photon transition probabilities and found that 2SM is in excellent agreement with the results from response theory. It is noticed that out of the donors and acceptors involved in study, D5 and A6 is the strongest donor, acceptor pair thereby giving large first and second hyperpolarizability making TSBD-13 a highly promising NLO material. We have noticed that all the molecules considered in the study are highly OP active whereas the second excited states of TSBD-1 to TSBD-6 are OP inactive. For the molecules from TSBD-7 to TSBD-13, the second excited state is OP active but with small values of oscillator strength. TSBD-11 is showing largest value of oscillator strength (1.790 a.u.). Our Λ -diagnosis and orbital analysis results clearly reveal the nature of transitions and their dependence on donor-acceptor combinations. TSBD-7 and TSBD-12 have shown maximum (0.695) and minimum (0.144) Λ values thereby indicated a clear short and long range charge transfer respectively. The molecules TSBD-1 to TSBD-6, TSBD-8, TSBD-9 and TSBD-11 have Λ values around 0.5 and show mixing of charge transfer and π -electron reorganization. The charge transfer from donor to acceptor is seen as the major contributing factor which is reflected by the dominance of S_{zz} as the molecules have been placed in yz -plane with donor and acceptor on z -axis. The relative trend followed by linear and NLOS and two-photon transition probabilities is similar. By applying 2SM approach to evaluate first hyperpolarizability and two-photon transition probability, we conclude that it is the $\Delta\mu^{ff}$ which is playing a major role in controlling the respective property values, where as the other factors have been seen moving out of trend several times. The TSB derivatives studied so far did not have TPA cross-section as high as we obtained (5560 G.M., $S_0 \rightarrow S_2$) for TSBD-13 by decorating it with suitable donor and acceptor. Other TSB derivatives TSBD-10, TSBD-11, TSBD-12 and TSBD-13 have also shown 1840 G.M., 1350 G.M., 2380 G.M. and 2270 G.M. σ_{TPA} values respectively for $S_0 \rightarrow S_1$ transition. We have noticed the strength of donor, acceptor and dipole moment difference between ground and excited states ($\Delta\mu^{ff}$) have been the main reasons for such large TP activity of TSBD-10, TSBD-11, TSBD-12 and TSBD-13. It is hoped that these can be synthesized experimentally and used as better photon manipulating materials in potential applications involving non-linear optics.

5 Acknowledgements

VK is thankful to the Ministry of Human Resources and Development (MHRD), Government of India, for his fellowship. The authors gratefully acknowledge Institute Computer Center (ICC), Indian Institute of Technology Roorkee (IITR), for providing access to their high performance computing (HPC)

facility and Dr. Navneet Kumar Gupta (System Programmer, ICC, IIT Roorkee) for his co-operation.

References

- (a) J. Kerr, *Phil. Mag.*, 1877, **3**, 321; (b) J. Kerr, *Phil. Mag.*, 1878, **5**, 161.
- F. T. Arecchi and E. O. Schulz-dubois, *Laser Handbook*, North-Holland, Amsterdam, 1972, vol. **1**.
- T. H. Maiman, *Nature*, 1960, **187**, 493.
- G. S. He, L. S. Tan, Q. Zheng and P. N. Prasad, *Chem. Rev.*, 2008, **108**, 1245-1330.
- M. Pawlicki, H. A. Collins, R. G. Denning and H. L. Anderson, *Angew. Chem., Int. Ed.*, 2009, **48**, 3244-3266.
- D. R. Kanis, M. A. Ratner and T. J. Marks, *Chem. Rev.*, 1994, **94**, 195.
- D. Li, T. J. Marks and M. A. Ratner, *J. Am. Chem. Soc.*, 1988, **110**, 1707.
- D. F. Eaton, G. R. Meridith and J. S. Miller, *Adv. Mater.*, 1992, **4**, 45.
- D. J. Williams, *Angew. Chem. Int. Ed. Engl.*, 1984, **23**, 690.
- B. F. Levine and C. G. Bethea, *Appl. Phys. Lett.*, 1974, **24**, 445.
- K. Clays and A. Persoons, *Phys. Rev. Lett.*, 1991, **66**, 2980.
- F. Wurthner, R. Wortmann and K. Meerholz, *ChemPhysChem*, 2002, **3**, 17.
- S. R. Marder, *Chem. Commun.*, 2006, **2**, 131.
- K. Y. Saponitsky, T. V. Timofeeva and M. Y. Antipin, *Russ. Chem. Rev.*, 2006, **75**, 457.
- L. R. Dalton, W. H. Steier, B. H. Robinson, C. Zhang, A. Ren, S. Garner, A. T. Chen, T. Londergan, L. Irwin, B. Carlsson, L. Fifield, G. Phelan, C. Kincaid, J. Amend and A. Jen, *J. Mater. Chem.*, 1999, **9**, 1905.
- D. L. I. Albert, T. J. Marks and M. A. Ratner, *J. Am. Chem. Soc.*, 1997, **119**, 6575-6582.
- K. Y. Saponitsky, S. Tafur and A. E. Masunov, *J. Chem. Phys.*, 2008, **129**, 044109.
- B. Skwara, W. Bartkowiak, A. Zawada, R. W. Gora and Leszczynski, *J. Chem. Phys. Lett.*, 2007, **436**, 116.
- Z. Benkova, I. Cernusak and P. Zahradnik, *Mol. Phys.*, 2006, **104**, 2011.
- M. Torrent-Sucarrat, M. Sola, M. Duran, J. M. Luis and B. Kirtman, *J. Chem. Phys.*, 2003, **118**, 711.
- T. Pluta and A. Sadlej, *J. Chem. Phys. Lett.*, 1998, **297**, 391.
- A. M. Masunov and S. Tretiak, *J. Phys. Chem. B*, 2004, **108**, 899.
- D. P. Shelton and J. E. Rice, *Chem. Rev.*, 1994, **94**, 3-29.
- B. Champagne, E. A. Perpète, D. Jacquemin, S. J. A.

- van Gisbergen, E. J. Baerends, C. Soubra-Ghaoui, K. A. Robins and B. Kirtman, *J. Phys. Chem. A*, 2000, **104**, 4755.
- 25 M. Gruning, O. V. Gritsenko, S. J. A. van Gisbergen and E. J. Baerends, *J. Chem. Phys.*, 2002, **116**, 9591.
- 26 A. J. Garza, G. E. Scuseria, S. B. Khan and A. M. Asiri, *Chem. Phys. Lett.*, 2013, **575**, 122-125.
- 27 O. A. Vydrov, J. Heyd, A. V. Krukau and G. E. Scuseria, *J. Chem. Phys.*, 2006, **125**, 074106.
- 28 O. A. Vydrov and G. E. Scuseria, *J. Chem. Phys.*, 2006, **125**, 234109.
- 29 D. Jacquemin, E. A. Perpte, O. A. Vydrov, G. E. Scuseria and C. Adamo, *J. Chem. Phys.*, 2007, **127**, 094102.
- 30 H. Iikura, T. Tsuneda, T. Yanai and K. Hirao, *J. Chem. Phys.*, 2001, **115**, 3540.
- 31 (a) P. A. Limacher, K. V. Mikkelsen and H. P. Luthi, *J. Chem. Phys.*, 2009, **130**, 194114. (b) D. H. Friese, M. T. P. Beerepoot, M. Ringholm and K. Ruud, *J. Chem. Theory Comput.*, 2015, **11**, 1129-1144. (c) D. H. Friese, C. Hattig and K. Ruud, *Phys. Chem. Chem. Phys.*, 2012, **14**, 1175-1184.
- 32 M. R. S. A. Janjua, S. Jamil, T. Ahmad, Z. Yang, A. Mahmood and S. Pan, *Comp. Theor. Chem.*, 2014, **1033**, 6-13.
- 33 S. G. Aziz, S. A. K. Elroby Jamil, R. H. Hilal, and O. I. Osman, *Comp. Theor. Chem.*, 2014, **1028**, 65-71.
- 34 (a) M. M. Alam, M. Chattopadhyaya and S. Chakrabarti, *J. Phys. Chem. A*, 2012, **116**, 11034-11040; (b) P. C. Jha, M. Das and S. Ramasesha, *J. Phys. Chem. A*, 2004, **108**, 6279-6285.
- 35 P. Krawczyk, *J. Mol. Model.*, 2010, **16**, 659-668.
- 36 L. T. Cheng, W. Tam, S. H. Stevenson and G. R. Meredith, *J. Phys. Chem.*, 1991, **95**, 10631-10643.
- 37 M. J. Frisch, G. W. Trucks, H. B. Schlegel, G. E. Scuseria, M. A. Robb, J. R. Cheeseman, G. Scalmani, V. Barone, B. Mennucci, G. A. Petersson et al., Gaussian, Inc., Wallingford CT, 2009.
- 38 K. Aidas, C. Angeli, K. L. Bak, V. Bakken, R. Bast, L. Boman, O. Christiansen, R. Cimraglia, S. Coriani, P. Dahle et al. *WIREs Comput. Mol. Sci.*, 2013, **4**, 269-284.
- 39 Dalton, a Molecular Electronic Structure Program, Release DALTON2013.4, 2014, see <http://daltonprogram.org>
- 40 J. Olsen and P. Jørgensen, *J. Chem. Phys.*, 1985, **82**, 3235-3264.
- 41 H. Hettema, H. J. Aa. Jensen, P. Jørgensen and J. Olsen, *J. Chem. Phys.*, 1992, **97**, 1174-1190.
- 42 T. Helgaker, S. Coriani, P. Jørgensen, K. Kristensen, J. Olsen and K. Ruud, *Chem. Rev.*, 2012, **112**, 543-631.
- 43 A. D. Becke, *J. Chem. Phys.*, 1993, **98**, 1372.
- 44 C. Lee, W. Yang and R. G. Parr, *Phys. Rev. B*, 1988, **37**, 785.
- 45 A. Willetts, J. E. Rice, D. M. Burland and D. P. Shelton, *J. Chem. Phys.*, 1992, **97**, 7590.
- 46 R. C. Hilborn, *Am. J. Phys.*, 1982, **50**, 982-986.
- 47 R. A. Rijkenberg, D. Bebelaar, W. J. Buma and W. J. Hofstra, *J. Phys. Chem. A*, 2002, **106**, 2446-2456.
- 48 P. N. Day, K. A. Nguyen and R. J. Pachter, *J. Chem. Phys.*, 2006, **125**, 094103-094113.
- 49 M. J. G. Peach, P. Benfield, T. Helgaker and D. J. Tozer, *J. Chem. Phys.*, 2008, **128**, 044118-044125.
- 50 M. M. Alam, M. Chattopadhyaya and S. Chakrabarti, *Phys. Chem. Chem. Phys.*, 2011, **13**, 9285-9292.
- 51 M. J. G. Peach, C. R. L. Sueur, K. Ruud, M. Guillaume and D. J. Tozer, *Phys. Chem. Chem. Phys.*, 2009, **11**, 4465-4470.
- 52 M. M. Alam, *Phys. Chem. Chem. Phys.*, 2014, **16**, 26342-26347.
- 53 V. Kundi, M. M. Alam and P. P. Thankachan *Phys. Chem. Chem. Phys.*, 2015, DOI: 10.1039/c5cp00026b.
- 54 M. J. Peach, A. J. Cohen and D. J. Tozer, *Phys. Chem. Chem. Phys.*, 2006, **8**, 4543-4549.
- 55 M. Chattopadhyaya, M. M. Alam and S. Chakrabarti, *J. Phys. Chem. A*, 2011, **115**, 2607-2614.
- 56 S. Chakrabarti and K. Ruud, *Phys. Chem. Chem. Phys.*, 2009, **11**, 2592-2596.
- 57 M. M. Alam, M. Chattopadhyaya and S. Chakrabarti, *Phys. Chem. Chem. Phys.*, 2012, **14**, 1156-1165.
- 58 M. M. Alam, M. Chattopadhyaya, S. Chakrabarti and K. Ruud, *J. Phys. Chem. Lett.*, 2012, **3**, 61-966.
- 59 (a) N. A. Murugan, J. Kongsted, Z. Rinkevicius, K. Aidas, K. V. Mikkelsen and H. Argen, *Phys. Chem. Chem. Phys.*, 2011, **13**, 12506-12516. (b) N. A. Murugan, J. Kongsted and H. Argen, *J. Chem. Theory Comput.*, 2013, **9**, 3660-3669. (c) N. A. Murugan, R. Apostolov, Z. Rinkevicius, J. Kongsted, E. Lindahl and H. Argen, *J. Am. Chem. Soc.*, 2013, **135**, 13590-13597.
- 60 A. Rizzo, S. Coriani and K. Ruud, in *Computational Strategies for Spectroscopy: from Small Molecules to Nano Systems*, ed. V. Barone, John Wiley & Sons, Hoboken, NJ, 2012, ch. 2, p. 77.
- 61 Y. R. Shen, *The Principles of Nonlinear Optics*, Wiley, New York, 1984, p. 23.
- 62 W. M. Clain, *J. Chem. Phys.*, 1971, **55**, 2789.
- 63 M. Jaszunski, A. Rizzo and K. Ruud, in *Handbook of Computational Chemistry*, ed. J. Leszczynski, Springer Science+Business Media, 1st edn, 2012, ch. 11, vol. **1**, p. 361.
- 64 P. N. Day, K. A. Nguyen and R. Pachter, *J. Phys. Chem. B*, 2005, **109**, 1803-1814.
- 65 P. N. Day, K. A. Nguyen and R. Pachter, *J. Chem. Phys.*, 2006, **125**, 094103.